Chapter 6

Friction, Ageostrophic Flow, and Oceans

In this chapter we complete our treatment of shallow water flow and apply the lessons we have learned to ocean circulations.

6.1 Ageostrophic flow

So far in our treatment of nearly balanced flows, we have assumed that the geostrophic velocity is a sufficiently accurate representation of the actual velocity. An examination of this approximation applied to the linearized continuity equation on an f-plane

$$\frac{\partial \eta}{\partial t} + \nabla \cdot \mathbf{v} = 0 \tag{6.1}$$

is enough to disprove this idea. Substituting the geostrophic velocity

$$v_{gx} = -\frac{c^2}{f}\frac{\partial \eta}{\partial y} \qquad v_{gy} = \frac{c^2}{f}\frac{\partial \eta}{\partial x} \tag{6.2}$$

into this equation and realizing that the Coriolis parameter f is constant on an f-plane, we get

$$\frac{\partial \eta}{\partial t} - \frac{c^2}{f}\frac{\partial^2 \eta}{\partial x \partial y} + \frac{c^2}{f}\frac{\partial^2 \eta}{\partial x \partial y} = \frac{\partial \eta}{\partial t} = 0, \tag{6.3}$$

i. e., the density field does not change with time!

Clearly this is incorrect. The continuity equation itself can be used to solve this problem. Let us assume that the actual velocity is the sum of geostrophic and *ageostrophic* parts, $\mathbf{v} = \mathbf{v}_g + \mathbf{v}_a$. In mathematical terms, the geostrophic wind is solenoidal, i. e., the divergence of the geostrophic wind is zero.

Any vector field can be split into solenoidal and irrotational parts. The divergence of the solenoidal part is (by definition) zero, while the curl of the irrotational part is zero. In order to satisfy the continuity equation, we postulate that the ageostrophic flow is irrotational but not solenoidal. Given this assumption, the ageostrophic part of the flow can be represented as the gradient of a potential:

$$\mathbf{v}_a = -\nabla \chi \tag{6.4}$$

The potential χ is called the *velocity potential.*

Substitution of equation (6.4) into equation (6.1) results in a diagnostic equation for χ:

$$\nabla^2\chi = \frac{\partial\eta}{\partial t}. \tag{6.5}$$

At first this equation appears less than useful, since the time derivative of the thickness perturbation is needed to solve for χ. However, recall that the time history of η is known from the repeated application of potential vorticity inversion at successive time steps. The thickness perturbation can therefore be approximated by a backward difference,

$$\frac{\partial\eta}{\partial t} \approx \frac{\eta(t) - \eta(t - \Delta t)}{\Delta t}. \tag{6.6}$$

Knowledge of the η field at the current and previous time steps is then sufficient to approximate $\partial\eta/\partial t$. This approximation becomes exact as $\Delta t \to 0$.

Solution of the quasi-balanced problem then proceeds conceptually in three rather than two steps:

1. Given the potential vorticity distribution at some time t, invert to obtain the thickness perturbation field and from this compute the geostrophic velocity.

2. Given the thickness perturbation at times t and $t - \Delta t$, approximate $\partial\eta/\partial t$ by equation (6.6) and solve for χ using equation (6.5). From χ compute the ageostrophic wind.

3. Use the sum of the geostrophic and ageostrophic flows to advect the potential vorticity distribution to the next time step. Repeat.

6.1.1 Simple ageostrophic flow example

We now apply this theory to a simple example, which is an extension of a problem previously studied. We postulate a potential vorticity perturbation on an f-plane of the form $q' = q_0 K t \delta(x)$ where $q_0 = f/h_0$ and K is a constant. This corresponds to strong strip of potential vorticity along the y axis which increases in magnitude with time. Inversion to obtain the thickness perturbation yields

$$\eta = -\frac{Kt}{2L_R}\exp(-|x|/L_R). \tag{6.7}$$

The geostrophic wind in this case is

$$v_{gx} = 0 \qquad v_{gy} = \frac{fKtx}{2|x|}\exp(-|x|/L_R) \tag{6.8}$$

Since $\partial^2\chi/\partial y^2 = 0$ by symmetry in this case, $v_{ax} = -\partial\chi/\partial x$ can be obtained by direct integration of equation (6.5). Since η is symmetric in x, v_{ax} is antisymmetric, which means that $v_{ax} = 0$ at $x = 0$. Thus, we find

$$v_{ax} = \frac{Kx}{2|x|}[1 - \exp(-|x|/L_R)] \qquad v_{ay} = 0. \tag{6.9}$$

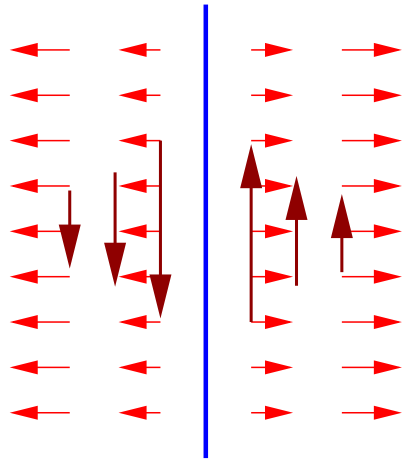

Figure 6.1: Flow pattern due to a vertical stripe of potential vorticity which is increasing with time. The vertical arrows represent the geostrophic flow while the horizontal arrows show the ageostrophic flow.

Note that since the ageostrophic wind is zero at $x = 0$ and the geostrophic wind is to the north and south, the pattern of potential vorticity does not change with time, and the potential vorticity evolution step is therefore trivial.

Figure 6.1 shows the geostrophic and ageostrophic flow resulting from the intensifying vertical strip of potential vorticity. Physically, as the potential vorticity increases, the thickness within about a Rossby radius of the potential vorticity strip decreases. The excess fluid has to go somewhere, so it oozes out to the left and the right like toothpaste in a tube open at both ends which is being squeezed in the center.

6.1.2 Geostrophic adjustment

At this point we note that while the balanced flow resulting from a given potential vorticity distribution and associated boundary conditions is unique, there are actually many *unbalanced* flows which result in the given potential vorticity distribution. This arises from the fact that the potential vorticity is determined by a combination of the vorticity distribution and the layer thickness distribution. Thus, any given potential vorticity pattern can be produced totally by the vorticity field or totally by the thickness field. An example of an unbalanced flow which results in the potential vorticity distribution discussed in the last section is shown in figure 6.2. The thickness is uniform and the vorticity is only non-zero in a strip along the y axis. The balance condition is actually a relationship between the thickness distribution and the velocity distribution, which in combination with the way thickness and vorticity produce potential vorticity, results in unique thickness and velocity fields.

As seen in the last section, when the potential vorticity pattern is evolving in time, the flow pattern is not quite balanced, but has a significant unbalanced or ageostrophic component. A snapshot of this process is shown in figure 6.3. The unbalanced Coriolis force acting on the flow on the right side of figure 6.2 tends to rotate the velocity vector clockwise, as illustrated in figure 6.3. The resulting flow away from the potential vorticity

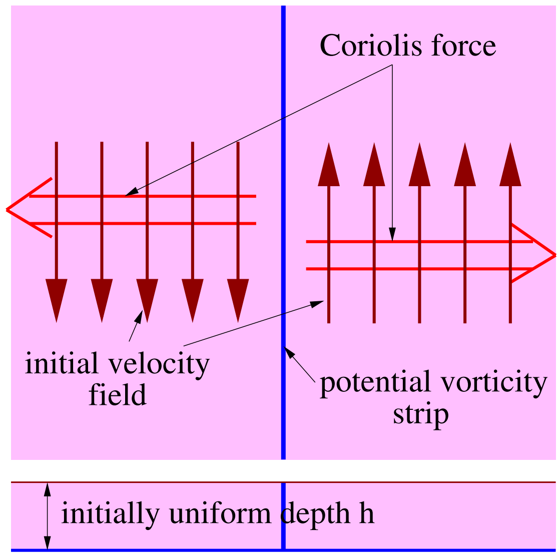

Figure 6.2: Unbalanced flow which produces a strip of potential vorticity along y axis equivalent to that shown in figure 6.1.

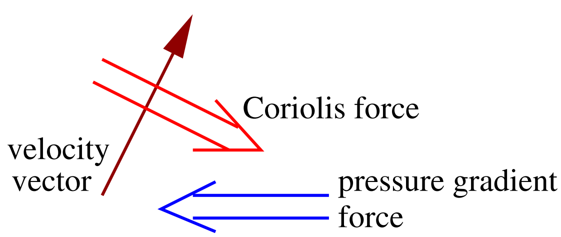

Figure 6.3: Evolving velocity, Coriolis force, and pressure gradient force to the right of the line of potential vorticity in figure 6.2.

strip evacuates fluid from the vicinity of the strip, reducing the layer thickness there. This produces a pressure gradient force back toward the strip, as shown in figure 6.3. Meanwhile, the y component of the Coriolis force tends to reduce the y velocity component at the same time that the pressure gradient force reduces the x component of the velocity. Eventually the mutual evolution of the velocity and thickness fields results in a steady, balanced flow pattern when the potential vorticity anomaly is constant in time. If the potential vorticity pattern is itself evolving, then this balanced state is never quite reached. However, the tendency of the ageostrophic flow in this case is to try to bring the overall flow into geostrophic balance. Often the difference between the actual flow and the balanced flow is relatively small.

6.2 Effects of friction

The effects of friction, and in particular the frictional drag imposed by the atmosphere, are key to understanding ocean circulation. We therefore incorporate friction our treatment of potential vorticity.

6.2.1 Forces on ocean surface layer

The primary driving force on the surface layer of the ocean is the atmospheric wind stress, expressed as a horizontal force per unit area of ocean surface, $\mathbf{T}$. This vector takes the approximate form

$$\mathbf{T} = \rho_a C_D |\mathbf{V}| \mathbf{V} \tag{6.10}$$

where ρ_a is the air density, $C_D \approx 1 - 2 \times 10^{-3}$ is the dimensionless *drag coefficient*, and $\mathbf{V}$ is the air velocity near the surface minus the ocean velocity, generally approximated as just the air velocity, since the ocean velocity is typically so much smaller. This formula has empirical origins, and C_D is generally a weak function of the wind speed.

Turbulent eddies distribute the effect of the surface stress through the depth of the surface layer in the ocean, and the effective force per unit mass is

$$\mathbf{F} = \frac{\mathbf{T}}{\rho_w h}, \tag{6.11}$$

where h is the depth of the surface layer.

Internal drag forces also operate between the ocean surface layer and deep water. These forces turn out to be quite important, but models for them are less well formulated than the atmospheric stress on the ocean surface.

6.2.2 Friction and potential vorticity

We previously discovered that the circulation theorem in a fluid of constant density in the presence of an external force $\mathbf{F}$ becomes

$$\frac{d\Gamma}{dt} = \oint \mathbf{F} \cdot d\mathbf{l} = \int \nabla \times \mathbf{F} \cdot \hat{\mathbf{n}} dA = \nabla \times \mathbf{F} \cdot \hat{\mathbf{n}} A \tag{6.12}$$

where we have in addition applied Stokes' theorem and assumed that the resulting surface integral can be approximated by a constant integrand value times the area bounded by the circulation loop.

Applying the circulation theorem to a horizontal loop in a shallow water flow allows us to replace the unit normal $\hat{\mathbf{n}}$ to the loop by the vertical unit vector $\hat{\mathbf{z}}$. Recall that the potential vorticity $q = \zeta_a/h = \Gamma/V$ where ζ_a is the vertical component of the absolute vorticity, h is the depth of the fluid, and $V = hA$ is the volume of the fluid element. The time derivative of the potential vorticity of a parcel under these conditions is

$$\frac{dq}{dt} = \frac{d}{dt}\left(\frac{\Gamma}{V}\right) = \frac{1}{V}\frac{d\Gamma}{dt} - \frac{\Gamma}{V^2}\frac{dV}{dt} = \frac{\nabla \times \mathbf{F} \cdot \hat{\mathbf{z}}}{h}. \tag{6.13}$$

The potential vorticity evolution equation thus becomes

$$\frac{\partial q}{\partial t} + \mathbf{v} \cdot \nabla q = \frac{\nabla \times \mathbf{F} \cdot \hat{\mathbf{z}}}{h}. \tag{6.14}$$

Equation (6.14) tells us that the potential vorticity of a parcel is increased if the z component of the curl of the applied force is positive. Clearly conservative forces, which have zero curl, have no effect on the potential vorticity distribution.

6.2.3 Simple example extended

We now hypothesize a simple force pattern of the form

$$\mathbf{F} = \frac{F_0 x}{|x|}\hat{\mathbf{y}}, \tag{6.15}$$

i. e., the force points in the y direction and changes sign at $x = 0$. The curl of the force is $\nabla \times \mathbf{F} = 2F_0\delta(x)\hat{\mathbf{z}}$ and potential vorticity evolution equation therefore takes the form

$$\frac{dq}{dt} = \frac{2F_0\delta(x)}{h}. \tag{6.16}$$

Assuming a uniform value of potential vorticity $q_0 = f/h_0$ everywhere but at $x = 0$, we find that

$$q' = q - q_0 = \frac{2F_0 t\delta(x)}{h}, \tag{6.17}$$

where we anticipate that the resulting fluid flow will simply advect potential vorticity along the y axis, which allows us to ignore the advection term $\mathbf{v} \cdot \nabla q$, since $\partial q/\partial y = 0$ in this case.

Comparison with the assumptions of section 6.1.1 shows us that we have precisely the same potential vorticity distribution in that case if we take $2F_0/h = q_0 K$. Further assuming that h undergoes only small fractional changes allows us to approximate h by h_0 in this equation, resulting in $K = 2F_0/f$. From equation (6.9) we see that the ageostrophic velocity resulting in this situation can be written in terms of the force as

$$v_{ax} = \frac{F_0 x}{f|x|}[1 - \exp(-|x|/L_R)] \qquad v_{ay} = 0, \tag{6.18}$$

or in other words, $v_{ax} = \pm F_y/f$ more than a few Rossby radii from the y axis, where η, and hence h, varies with position.

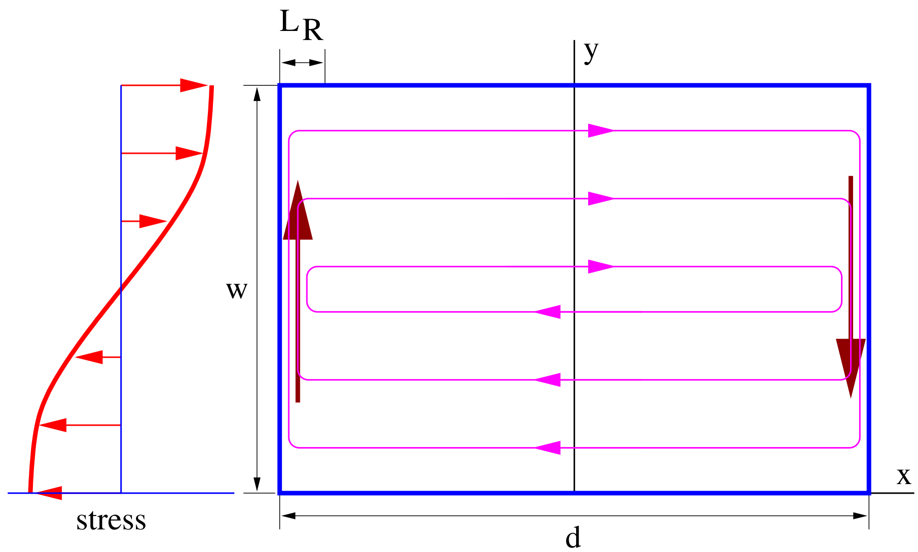

Figure 6.4: Idealized ocean basin with sinusoidal east-west wind stress.

6.3 Ocean currents

We now explore several examples of real phenomena in the oceans, and how our newly developed tools can be used to understand them.

6.3.1 Wind stress and ocean gyres – f-plane

Let us consider a highly idealized model of an ocean basin with a zonal (east-west) atmospheric wind stress acting on it, as illustrated in figure 6.4. The wind stress pattern is meant to represent approximately that actually found in the northern hemisphere, with surface westerly winds (i. e., *from* the west according to meteorological convection) north of about 30° N and easterly winds south of this latitude. We represent this stress by the cosine function

$$\mathbf{T} = -T_0 \cos(\pi y/w)\hat{\mathbf{x}}, \tag{6.19}$$

where T_0 is a constant. Assuming that the depth of the surface layer of the ocean is $h = h_0(1+\eta)$ where $|\eta| \ll 1$ as usual, we approximate the force per unit mass in the surface layer due to the wind stress as $\mathbf{F} = \mathbf{T}/(\rho_w h_0)$. The z component of the curl of this force is $\nabla \times \mathbf{F} = -[\pi T_0/(\rho_w w h_0)]\sin(\pi y/w)$, and so the potential vorticity evolution equation is

$$\frac{\partial q^*}{\partial t} + \mathbf{v}\cdot\nabla q^* = -\frac{\pi T_0}{\rho_w w h_0^2}\sin(\pi y/w). \tag{6.20}$$

where $q = q_0 + q^*$, with $q_0 = f_0/h_0$ as usual.

The perturbation potential vorticity contains a planetary part due to the variation of Coriolis parameter with latitude, and a part due to the motion of the system. Let us initially assume an f-plane, so that the latitudinal variability of the planetary part of the potential vorticity is suppressed. This is highly unrealistic, but the solution to this problem sets the stage for the more complex beta plane case. In this situation the advection term

$\mathbf{v} \cdot \nabla q^*$ is nonlinear in quantities having to do with the flow of the ocean, and can therefore be neglected in the initial small-amplitude evolution of the ocean circulation which occurs shortly after the surface stress is turned on. In this case we have

$$q^* = -\frac{\pi T_0 t}{\rho_w w h_0^2} \sin(\pi y/w), \tag{6.21}$$

i. e., the potential vorticity initially just decreases in place due to the pattern of wind stress.

The inversion equation for the thickness perturbation is

$$L_R^2 \nabla^2 \eta - \eta = \frac{q^*}{q_0} = -\frac{\pi T_0 t}{\rho_w w h_0 f_0} \sin(\pi y/w) \equiv -\epsilon \sin(\pi y/w), \tag{6.22}$$

where we have encapsulated the expression multiplying the sine function into the single variable ϵ. The solution to equation (6.22) can be divided into inhomogeneous and homogeneous parts, $\eta = \eta_I + \eta_H$. The inhomogeneous part can be written $\eta_I = \eta_{I0} \sin(\pi y/w)$, where $\eta_{I0} = \epsilon/(1 + \pi^2 L_R^2/w^2)$.

We now need to choose a homogeneous solution, i. e., one with ϵ set to zero in equation (6.22), which together with the inhomogeneous solution satisfies the boundary conditions of no flow through the side walls of the ocean basin. Technically, we need to arrange for the normal component of the sum of the geostrophic and ageostrophic flows to be zero on each side wall. However, since the ageostrophic part of the flow is generally small compared with the geostrophic part, we settle for the technically less demanding condition that the component of the geostrophic velocity normal to the boundary be zero there. This condition is satisfied by requiring that $\eta = 0$ everywhere on the boundary.

A solution satisfying this condition is

$$\eta_H = \eta_{H0}\{\exp[-\sigma(x + d/2)] + \exp[\sigma(x - d/2)]\} \sin(\pi y/w), \tag{6.23}$$

where

$$\eta_{H0} = -\frac{\epsilon}{(1 + \pi^2 L_R^2/w^2)[1 + \exp(-\sigma d)]} \tag{6.24}$$

and where

$$\sigma = \left(\frac{\pi^2}{w^2} + \frac{1}{L_R^2}\right)^{1/2}. \tag{6.25}$$

Recall that the oceanic Rossby radius for the internal mode is of order 50 km, whereas typical ocean basin dimensions (d and w) are thousands of kilometers. This leads to the simplifications that $\eta_{H0} \approx -\epsilon w^2/(\pi L_R)^2$ and $\sigma \approx 1/L_R$.

Contours of constant η are shown in figure 6.4, with arrows showing the flow pattern. The surface layer is thicker in the center of the ocean, consonant with the negative potential vorticity perturbation there. Arrows show the resulting geostrophic flow, which in the interior of the ocean basin tends to follow the pattern of surface stress. However, within a few Rossby radii of the east and west coasts the regime is quite different, with strong thickness gradients and correspondingly strong *coastal jets*, moving southward on the eastern boundary and northward on the western boundary in the northern hemisphere. The circulation in the southern hemisphere has the opposite sense due to the negative value of f_0 there.

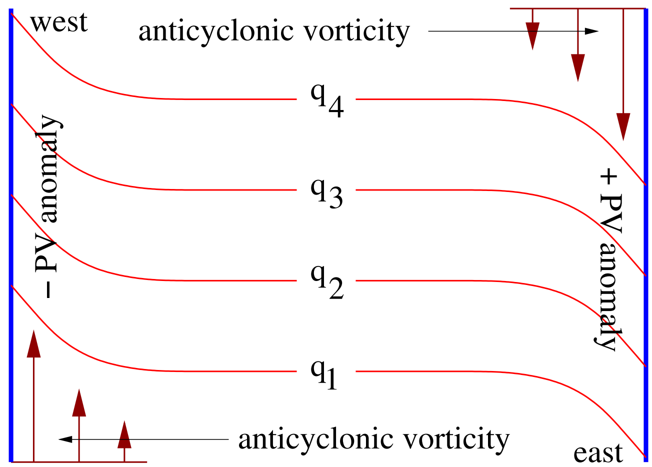

Figure 6.5: Effect of eastern and western boundary currents on potential vorticity distribution. The potential vorticity contours have $q_4 > q_3 > q_2 > q_1$, so that the advection due to the boundary currents causes a positive potential vorticity anomaly in the eastern boundary current and a negative anomaly in the western current.

As indicated, this solution is only valid for small amplitudes. As the circulation builds up under continuing wind stress, nonlinear effects eventually begin to modify the solution. Ultimately dissipation must begin to counteract the continual buildup of energy in the ocean circulation.

6.3.2 Wind stress and ocean gyres – beta-plane

The initial solution for the case of latitudinally varying Coriolis parameter is identical to the f-plane case. The beta effect only enters when advection of potential vorticity becomes significant. Nonlinear effects enter much earlier in the beta-plane case than for an f-plane, and following the detailed evolution of the flow becomes difficult or impossible. However, it is possible to make significant inferences about the final, equilibrium state of the flow.

In order to get at least a qualitative picture of how the flow evolves in the presence of the beta effect, notice how the eastern and western boundary currents advect the potential vorticity, resulting in a positive potential vorticity anomaly in the eastern current and a negative anomaly in the western current. Both currents have anticyclonic relative vorticity. In the eastern boundary current the positive potential vorticity anomaly creates a positive relative vorticity anomaly, which opposes the relative vorticity anomaly in the jet, reducing the jet strength. Eventually the positive anomaly increases sufficiently to cancel the negative anomaly completely, and the eastern boundary current comes to a halt. On the other hand, the negative potential vorticity anomaly in the western boundary current produces a negative relative vorticity anomaly which reinforces the anomaly pre-existing in the jet. This strengthens the jet, which increases the potential vorticity anomaly, which further strengthens the jet, etc., resulting in a runaway situation.

The kinks in the potential vorticity contours produced in the eastern boundary current propagate to the west as Rossby waves. Rossby wave adjustment continues until the contours

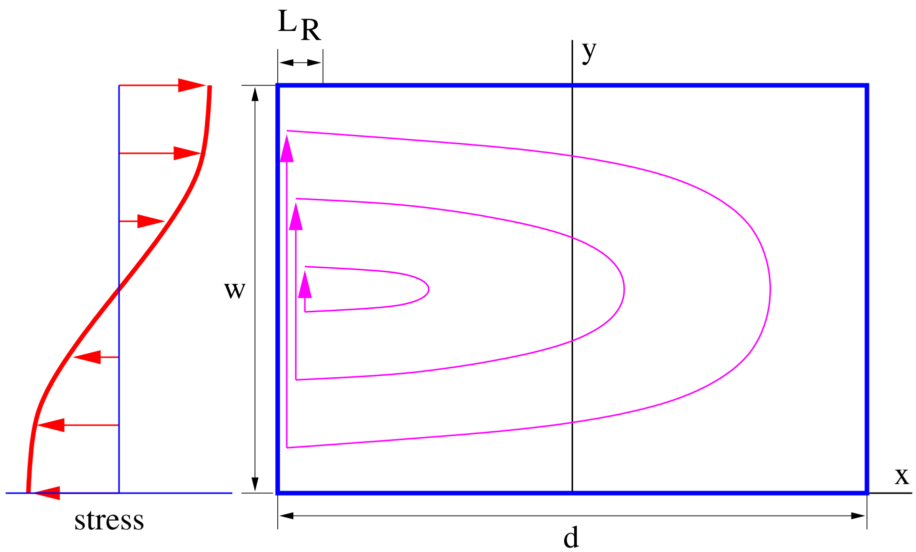

Figure 6.6: Idealized ocean circulation with the illustrated stress. Sverdrup flow occurs in the interior and eastern boundary, whereas western boundary current dynamics applies within a few Rossby radii of the western boundary.

become aligned perfectly east-west everywhere except for the western boundary region, where the very strong jet there does not allow equilibration to occur.

When a steady situation is reached everywhere except near the western boundary, the decrease in potential vorticity due to the wind stress curl is counterbalanced by a southward flow. This balance is called *Sverdrup balance* after the Norwegian oceanographer who developed the theory of this phenomenon. In terms of the potential vorticity advection equation, the balance is expressed

$$v_y \frac{\partial q}{\partial y} = \left(\frac{\partial q^*}{\partial t} \right)_{stress} = -\frac{\pi T_0}{\rho_w w h_0^2} \sin(\pi y/w) \tag{6.26}$$

where q^* is obtained from equation (6.21). Assuming that the thickness of the surface layer does not change much over the ocean, we have $q \approx q_0 + \beta y/h_0$, and the drift velocity is

$$v_y = -\frac{\pi T_0}{\rho_w w h_0 \beta} \sin(\pi y/w). \tag{6.27}$$

Since the y component of the flow is specified everywhere, the x component can be obtained from the continuity equation, again assuming that $h \approx h_0$. In this case the steady state continuity equation is

$$\frac{\partial v_x}{\partial x} + \frac{\partial v_y}{\partial y} = 0. \tag{6.28}$$

This may be integrated in x to obtain

$$v_x = \frac{\pi^2 T_0 (x - d/2)}{\rho_w w^2 h_0 \beta} \cos(\pi y/w), \tag{6.29}$$

where we have set the constant of integration (which is actually a function of y) so that $v_x = 0$ at the eastern boundary as defined in figure 6.4. Notice that $v_x \neq 0$ at the western boundary. This is because the solution is not valid in the western boundary region itself. In effect, the east-west velocity adjacent to the boundary current serves as a mass sink-source for the current. The resulting circulation is illustrated in figure 6.6.

Comparison with actual ocean circulations shows good agreement with Sverdrup flow and the implied western boundary current flow from the subtropics north to near the axis of the mid-latitude westerly winds. North of this nonlinear effects enter strongly, resulting in a complex, time-dependent structure for the western boundary current.

The real significance of western boundary currents from our point of view is that they transport large quantities of warm water from the subtropics to high latitudes. They are thus key elements in the redistribution of solar heating. The unit of transport volume transport in the ocean is named after Sverdrup: 1 Sv $= 10^6$ m^3 s^{-1}. The Gulf Stream, which is a western boundary current off the east coast of the United States, transports approximately 25 Sv of water from the Gulf of Mexico into the north Atlantic. Further north the transport is even greater.

6.4 Problems

1. Given the solution for a Rossby wave ($L_R = 1$, $f = 1$) in a channel with tilted bottom, $\eta = -\mu y + \eta_0 \sin(\pi y/w)\cos(kx - \omega t)$, with $\omega = -\mu k/(1 + k^2 + \pi^2/w^2)$, compute the ageostrophic wind by taking the following steps:

   (a) Compute the inhomogeneous solution to the velocity potential χ equation $\nabla^2\chi = \partial\eta/\partial t$. Hint: Assume that $\chi = F(y)\sin(kx - \omega t)$ where $F(y)$ is a function of y alone, so that $\partial^2\chi/\partial x^2 = -k^2\chi$, thus simplifying $\nabla^2\chi$.

   (b) Notice that the trial ageostrophic wind computed from the inhomogeneous part of the velocity potential does not satisfy the boundary conditions $v_{ay} = -\partial\chi/\partial y = 0$ at $y = 0, w$. Find the homogeneous solution to the velocity potential equation which, when added to the inhomogeneous solution, results in an ageostrophic wind which satisfies these boundary conditions. Hint: Note that the equation for the homogeneous part of F is

   $$\frac{d^2F}{dy^2} - k^2F = 0.$$

   This has real exponentials as solutions. Given the symmetry of the problem, try a solution of the form $A\exp[-ky] + B\exp[k(y-w)]$ where A and B are constants to be adjusted to satisfy the boundary conditions.

2. Sverdrup drift and the Gulf Stream:

   (a) Putting in reasonable values for the dimensions of the Atlantic Ocean, the depth of the upper oceanic layer (try 100 m), and the strength of the wind stress, estimate mass of water per unit time drifting south at the latitude of maximum anticyclonic wind stress curl. This equals the northward mass transport in the Gulf Stream at that latitude. Make a reasonable estimate for the maximum wind stress T_0.

(b) Assuming that the Gulf Stream is one Rossby radius wide, what is the estimated northward flow velocity in the Gulf Stream? Note that the Rossby radius in this case should be based on the equivalent depth rather than the actual depth of the layer, since the entire oceanic gyre is an internal mode involving mainly motions in the upper oceanic layer.

3. If the Gulf Stream is 10° C warmer than the main body of the upper ocean, use the results of the above problem to estimate the net northward transport of heat due to the ocean gyre, of which the Gulf Stream is the northward branch. Compare this result to the actual meridional ocean transport of heat. Hint: This transport is equal to the mass per unit time transported by the Gulf Stream times the difference in the internal energy content per unit mass between the northward-flowing Gulf Stream and the main body of the upper ocean.